PHYSICAL REVIEW B **91**, 195131 (2015)

Topological paramagnetism in frustrated spin-1 Mott insulators

Chong Wang, Adam Nahum, and T. Senthil
Department of Physics, Massachusetts Institute of Technology, Cambridge, Massachusetts 02139, USA
(Received 14 January 2015; revised manuscript received 6 April 2015; published 20 May 2015)

Time-reversal-protected three-dimensional (3D) topological paramagnets are magnetic analogs of the celebrated 3D topological insulators. Such paramagnets have a bulk gap and no exotic bulk excitations, but have non-trivial surface states protected by symmetry. We propose that frustrated spin-1 quantum magnets are a natural setting for realizing such states in three dimensions. We describe a physical picture of the ground-state wave function for such a spin-1 topological paramagnet in terms of loops of fluctuating Haldane chains with nontrivial linking phases. We illustrate some aspects of such loop gases with simple exactly solvable models. We also show how 3D topological paramagnets can be very naturally accessed within a slave particle description of a spin-1 magnet. Specifically, we construct slave-particle mean-field states which are naturally driven into the topological paramagnet upon including fluctuations. We propose bulk projected wave functions for the topological paramagnet based on this slave-particle description. An alternate slave-particle construction leads to a stable U(1) quantum spin liquid from which a topological paramagnet may be accessed by condensing the emergent magnetic monopole excitation of the spin liquid.

DOI: 10.1103/PhysRevB.91.195131 PACS number(s): 75.10.Kt, 75.10.Jm, 75.45.+j, 71.27.+a

I. INTRODUCTION

Frustrated quantum magnets display a rich variety of many-body phenomena. Some such magnets show long-range magnetic order at low temperature, often selected out of a manifold of degenerate classical ground states by quantum fluctuations. A very interesting alternative possibility, known as quantum paramagnetism, is the avoidance of such ordering even at zero temperature. Quantum paramagnets may be of various types. A fascinating and intensely studied class is the quantum spin liquids: these display many novel phenomena, for instance, fractionalization of quantum numbers and topological order, or gapless excitations that are robust despite the absence of broken symmetries [1–3].

Recently, there has been much progress in understanding a different type of remarkable quantum paramagnet. These are phases which have a bulk gap and no fractional quantum numbers or topological order. Despite this, they have nontrivial surface states that are protected by global symmetries. These properties are reminiscent of the celebrated electronic topological band insulators. Hence they have been called topological paramagnets [4]. Topological paramagnets and topological band insulators are both examples of what are known as symmetry-protected topological (SPT) phases [5–7]. A classic example of a topological paramagnet is the Haldane/Affleck-Kennedy-Lieb-Tasaki (AKLT) spin-1 chain: although this has a bulk gap and no bulk fractionalization, it has dangling spin-1/2 moments at the edge which are protected by symmetry, for instance, time reversal. In the last few years tremendous progress has been made in understanding such SPT phases and their physical properties in various dimensions (for reviews, see Refs. [8,9]).

The main focus of the present paper is on three-dimensional topological paramagnets that are protected by time reversal (we also briefly discuss topological paramagnets protected by other symmetries, notably conservation of at least one spin component). These are interesting for a number of reasons. First, time reversal is a robust symmetry of typical physical spin Hamiltonians. In one dimension the familiar Haldane/AKLT chain is the only time-reversal-protected topological paramagnet, while in two dimensions there are no time-reversal-protected topological paramagnets. In three dimensions, however, there are three distinct nontrivial phases [4,10,11] (corresponding to a classification by the group $\mathbb{Z}_2^2$). Second, regarded as an *electronic* insulator, unlike the 1D Haldane chain [12], these three-dimensional (3D) topological paramagnets survive as distinct interacting SPT insulators [13]. The properties and experimental fingerprints of such topological paramagnets were described in Refs. [4,10,11,13]. However, there is currently very little understanding of where such phases might actually be found. In this paper we propose that frustrated spin-1 Mott insulators may be good places to look for an example of such phases.

Already in the familiar one-dimensional (1D) example it is the spin-1 antiferromagnetic chain, rather than the spin-1/2 chain, that naturally becomes a topological paramagnet. In three dimensions for one of the topological paramagnets we provide a physical picture and a parton construction which are both very natural for the spin-1 case. We hope that our observations inspire experimental and numerical studies of frustrated spin-1 quantum magnetism in the future. Towards the end of the paper we remark on materials that may form such interesting frustrated magnets.

The three 3D topological paramagnets that are protected by time-reversal symmetry alone [4,10,11] all allow for a gapped surface with $\mathbb{Z}_2$ topological order (i.e., a gapped surface $\mathbb{Z}_2$ quantum spin liquid) even though the bulk itself is not topologically ordered. The properties of this *surface* theory give a useful way to label the bulk phases. The surface has gapped quasiparticle excitations, labeled e and m, which are mutual semions. These may be thought of as the electric charge and magnetic flux of a deconfined $\mathbb{Z}_2$ gauge theory (like the vertex and plaquette defects of Kitaev's toric code [14]). At the SPT surfaces these particles have self-statistics or time-reversal transformation properties that are impossible in a strictly two-dimensional (2D) system and that encode the

topology of the bulk wave function. The three nontrivial bulk states are denoted

$$eTmT, \quad efTmfT, \quad efmf.$$

In the first and second, the surface e and m excitations are each Kramers doublets under time reversal, denoted by T. In the second and third they are fermions f, while in the first they are bosons. This paper focuses primarily on the $eTmT$ state.

We begin by explaining a physical picture of a suitable ground-state wave function for the $eTmT$ topological paramagnet. This is most easily visualized on a diamond lattice. We first close pack each interpenetrating fcc sublattice of the diamond lattice with closed loops. On each loop we place all the spin-1 moments (located at the diamond sites) in the ground state of the 1D AKLT chain. We then superpose all such loop configurations with a crucial (-1) sign factor whenever loops from the two different fcc sublattices link. We argue that this construction yields the topological paramagnet.

To understand the topological properties of such a wave function we describe a simple exactly solvable loop-gas Hamiltonian [15], equivalent to two coupled Ising gauge theories, that clarifies the role of the $(-1)^{\text{linking}}$ sign structure. In this solvable model the loops do not have AKLT cores, but there are two species of loops on different sublattices with the mutual (-1) linking sign. It demonstrates very simply how this sign leads to a state without intrinsic topological order. (This loop gas is not in the $eTmT$ state because of the absence of AKLT cores, but we show it to be nontrivial in a different sense.)

Next, we use the two-orbital fermionic parton representation developed for spin-1 magnets [16] to construct possible ground states. When the fermionic partons have the mean-field dispersion of a certain topological superconductor, we show that the gauge fluctuations associated with the parton description convert the system into a topological paramagnet. In this construction the mean-field state is *unstable* toward confinement by gauge fluctuations as a result of a continuous non-Abelian gauge symmetry. Despite this the bulk gap survives, leaving behind a nontrivial surface that we are able to identify as that of the $eTmT$ topological paramagnet. As a warm-up exercise to illustrate some of the ideas of this 3D construction, we also describe how to access the 1D Haldane phase by confining a topological superconductor of parton fermions. The 3D construction naturally suggests alternative bulk wave functions for topological paramagnets, in the form of Gutzwiller-projected topological superconductors. This may be fruitful for future numerical work on the energetics of microscopic models.

This parton construction also gives access to other SPT states for quantum magnets in three dimensions. For instance, we show how to naturally obtain an SPT paramagnet (dubbed $eCmT$ in Ref. [10]) protected by $\mathrm{U}(1) \times \mathbb{Z}_2^T$, where U(1) describes rotation about one spin axis, say S_z, and $\mathbb{Z}_2^T$ is time reversal.

Finally, we show how to access a bulk U(1) quantum spin liquid with nontrivial implementation of time-reversal symmetry. Interestingly, simply condensing the magnetic monopole of this U(1) spin liquid leads to an SPT state dubbed $eCTmT$ in the presence of both spin rotation and time-reversal symmetries. If only time reversal is present, this becomes the $eTmT$ state.

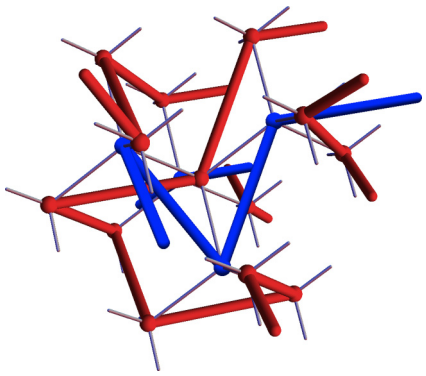

FIG. 1. (Color online) Two species of AKLT loops, one on each sublattice of the diamond lattice (blue and red). Note that loops live on the links of the fcc sublattices, i.e., on next-nearest-neighbor bonds of diamond.

II. LOOP-GAS STATES

In this section we describe a loop-gas wave function that is naturally adapted to spin-1 magnets and gives an intuitive picture for the $eTmT$ state. The wave function is a superposition of loop configurations, with each loop representing an AKLT state [17] for the spins lying on it. A given configuration enters the superposition with a sign factor determined by its topology: specifically, the loops come in two species, A and B (one associated with each sublattice of the bipartite diamond lattice), and the sign depends on the linking number of A loops with B loops (see Fig. 1). This geometrical picture makes the relationship between the bulk wave function and the surface excitations particularly simple. The surface e and m excitations are end points of the two species of AKLT chains and are Kramers doublets since an AKLT chain has dangling spin-1/2s at its ends.

In Sec. III we describe a similar wave function for "pure loops," i.e., loops that do not carry an internal AKLT structure. This may be regarded as a state of two coupled Ising gauge theories. It is *not* in the $eTmT$ phase, but it illustrates the basic features of the loop gases in a simple model with an exactly solvable Hamiltonian. This pure-loop model is also interesting in its own right: when open strands (as opposed to closed loops) are banished from the Hilbert space, i.e., when charge is absent, it is in a nontrivial phase despite the absence of topological order. Therefore it may be viewed as a "constraint-protected" state. It would be interesting to relate this to the recent ideas of Ref. [18]. We note that the constrained models discussed in Ref. [19] are also believed to be separated from the trivial phase by a phase transition, despite the absence of topological order.

The wave functions discussed here are in a similar spirit to the Walker Wang models, which are formulated in terms of string nets with a nontrivial sign structure, and show bulk confinement and surface topological order [11,20,21]. Constructions of SPTs using Walker Wang models were given in Refs. [11,22]. Two-dimensional "symmetry-enriched" topological states [23–25] and SPT states [26] have also been constructed by attaching AKLT chains to looplike degrees of freedom (see also [27]).

A. Fluctuating AKLT chains

The diamond lattice is made up of two fcc sublattices, A and B. If $\mathcal{C}_A$ is a configuration of fully packed loops on A (with every A site visited by exactly one loop), we define $|\mathcal{C}_A\rangle$ to be a product of AKLT states $|\mathcal{L}\rangle$ for each of the loops $\mathcal{L}$ in $\mathcal{C}_A$,

$$|\mathcal{C}_A\rangle = \prod_{\mathcal{L}\in\mathcal{C}_A} |\mathcal{L}\rangle\,. \tag{1}$$

Similarly, $|\mathcal{C}_B\rangle$ is the state corresponding to a loop configuration $\mathcal{C}_B$ on B. To define the AKLT states $|\mathcal{L}\rangle$ fully we must choose an orientation for the fcc links, as discussed below (Sec. II B).

Let $X(\mathcal{C}_A,\mathcal{C}_B)$ be the mutual linking number of the two species of loops. Since the loops are unoriented, this is defined modulo 2: $X(\mathcal{C}_A,\mathcal{C}_B) = 0,1$. A schematic wave function for the $eTmT$ phase may be written in terms of $X(\mathcal{C}_A,\mathcal{C}_B)$:

$$|\Phi\rangle = \sum_{\mathcal{C}_A,\mathcal{C}_A} (-1)^{X(\mathcal{C}_A,\mathcal{C}_B)}\,|\mathcal{C}_A\rangle\,|\mathcal{C}_B\rangle\,. \tag{2}$$

For concreteness, we take periodic boundary conditions. The sums over $\mathcal{C}_A$ and $\mathcal{C}_B$ are then each restricted to loop configurations with an *even* number of strands winding around the 3D torus in each direction, for reasons discussed below. This global constraint, together with the geometrical fact that the links of A never intersect those of B, ensures that $X(\mathcal{C}_A,\mathcal{C}_B)$ is well defined.

The entanglement between the two sublattices in Eq. (2) is entirely due to the sign factor. First, consider what happens in the *absence* of this sign factor. Each sublattice then hosts a superposition of loop configurations with positive amplitude, e.g., $\sum_{\mathcal{C}_A}|\mathcal{C}_A\rangle$. By analogy with the usual picture of deconfined $\mathbb{Z}_2$ gauge theory as a superposition of electric flux loop configurations [28], we would expect such a state to show $\mathbb{Z}_2$ topological order. (It is a 3D version of the "resonating AKLT" states studied in two dimensions [23–25].) The end point of an open AKLT chain is the deconfined $\mathbb{Z}_2$ charge in this state. Associated with the topological order is ground-state degeneracy: different ground states are distinguished by the parity of the winding number in each spatial direction.

In contrast, $|\Phi\rangle$ is *not* expected to show topological order, despite the proliferation of long loops in Eq. (2). Instead, it describes a phase in which the end points of open chains are confined in the bulk. Furthermore there is no ground-state degeneracy: states with odd winding numbers are not ground states (i.e., are not locally indistinguishable from $|\Phi\rangle$).

More detailed discussion of this is deferred for the solvable model of Sec. III, but the basic idea is the following. While the amplitude $(-1)^{X(\mathcal{C}_A,\mathcal{C}_B)}$ depends on the *global* topology of the loop configurations, it amounts to the simple *local* rule that the amplitude changes sign if an A strand is passed through a B strand. It is useful to imagine a hypothetical parent Hamiltonian that imposes this sign rule. But the sign rule cannot be consistently imposed if the wave function includes open strands or configurations with odd winding numbers (see below). Similar phenomena occur in the confined Walker-Wang models [11,20,21].

However, open end points are deconfined at the boundary for appropriate boundary conditions. The minus sign associated with passing an A strand through a B strand in the bulk means that the end points are mutual semions [29] (see Fig. 2). They are also Kramers doublets. These surface properties are the defining features of the $eTmT$ state. The wave function $|\Phi\rangle$ has more symmetry than simply time reversal (e.g., separate spin-rotation symmetries for each sublattice), but if it is indeed in the $eTmT$ phase, then these symmetries could be weakly broken without leaving the phase.

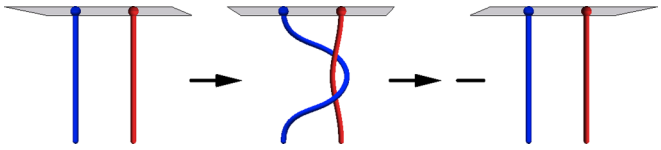

FIG. 2. (Color online) For appropriate boundary conditions, end points of A and B chains (red and blue, respectively) give surface excitations with mutual semionic statistics. Braiding the anyons on the surface (first arrow) changes the sign of the wave function for consistency with the rule that configurations related by passing an A strand through a B strand in the bulk (second arrow) appear in the wave function with opposite sign.

B. Further details on fluctuating AKLT state

To write the AKLT-based state explicitly it is convenient to represent the spin-1 at each site i in terms of auxiliary spin-1/2 bosons [17,27]. If the boson creation operators are $b^\dagger_{i\alpha}$ ($\alpha = \uparrow,\downarrow$), then $\vec{S}_i = \frac{1}{2} b^\dagger_{i\alpha}\vec{\sigma}_{\alpha\beta}b_{i\beta}$. The occupation number $b^\dagger_{\alpha i}b_{i\alpha}$ is equal to 2 to ensure spin-1 at each site. The AKLT state $|\mathcal{L}\rangle$ is then created by acting on the boson vacuum with operators $S^\dagger_{ij}$ that create singlet pairs on the links of the loop, which we normalize as $S^\dagger_{ij} = \frac{1}{\sqrt{3}}(b^\dagger_{i\uparrow}b^\dagger_{j\downarrow} - b^\dagger_{i\downarrow}b^\dagger_{j\uparrow})$. This operator is antisymmetric in (i,j), so to define $|\Phi\rangle$ we must fix an orientation for the links of each fcc sublattice. (The fcc lattice has four sublattices, a,b,c,d, so, for example, we could orient the links from $a\to b$, $a\to c$, $a\to d$, $b\to c\to d\to b$, with the orientations on each sublattice related by inversion symmetry.) Then for each sublattice

$$|\mathcal{C}\rangle = \prod_{\langle ij\rangle\in\mathcal{C}} S^\dagger_{ij}\,|\mathrm{vac}\rangle\,, \tag{3}$$

where i is the site at the tail of the oriented link $\langle ij\rangle$. These states satisfy $\langle\mathcal{C}|\mathcal{C}\rangle = \prod_{\mathrm{loops}}(1+(-1)^\ell/3^{\ell-1})$, where ℓ is the length of a given loop [17].

It should be noted that that expectation values in the state $|\Phi\rangle$ are nontrivial, in particular because overlaps $\langle\mathcal{C}|\mathcal{C}'\rangle$ for distinct $\mathcal{C},\mathcal{C}'$ are nonzero. So while it is plausible that $|\Phi\rangle$ is in the $eTmT$ phase, this cannot be established purely analytically. For example, the state could, in principle, break spatial or spin-rotation symmetry spontaneously. A cautionary example is given by the uniform-amplitude resonating valence-bond state for spin-1/2s on the cubic lattice: this has weak Néel order [30], despite being a superposition of singlet configurations which individually have trivial spin correlations. In the present model, the entanglement between sublattices suppresses off-diagonal elements of the reduced density matrix when written in the AKLT-chain basis [31]. Together with the nonbipartiteness of the fcc lattice, this makes spin order seem less likely. But

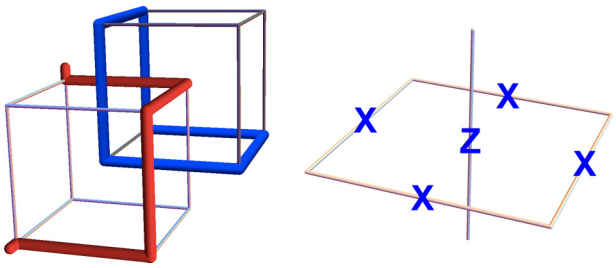

FIG. 3. (Color online) (left) Loops on interpenetrating cubic lattices A and B. State $|\Psi\rangle$ is a superposition of such configurations with signs determined by linking A and B loops. (right) The product of Pauli matrices defining the flip term $\mathcal{F}$ on a plaquette [see Eq. (6)].

since $|\Phi\rangle$ is intended to illustrate the topological structure of the phase and not as a ground state of a realistic Hamiltonian, it may not be crucial whether it is in the desired phase as written or whether further tuning of the amplitudes is required.

III. PURE-LOOP STATE

It is enlightening to look at the simplest model [15] that captures the $(-1)^{\text{linking}}$ sign structure. To this end we take a system of spin-1/2s on the *links* of two interpenetrating cubic lattices A and B, as shown in Fig. 3. We think of a down spin (in the z basis) as an occupied link and an up spin as an unoccupied one. The number of occupied links at each vertex is always even in the state we consider, so the configurations of occupied links, $\mathcal{C}_A$ and $\mathcal{C}_B$, can be decomposed into closed loops [32]. We refer to $\mathcal{C}_A$ and $\mathcal{C}_B$ as loop configurations. Other solvable loop-gas/string-net models have been considered in Refs. [11,21], using the Walker-Wang construction [20].

The pure-loop state analogous to $|\Phi\rangle$ above is (again we sum only over loop configurations with even winding numbers on each sublattice)

$$|\Psi\rangle = \sum_{\mathcal{C}_A,\mathcal{C}_B} (-1)^{X(\mathcal{C}_A,\mathcal{C}_B)} |\mathcal{C}_A\rangle\, |\mathcal{C}_B\rangle\,. \tag{4}$$

We may view $\mathcal{C}_A$ and $\mathcal{C}_B$ as the electric flux-line configurations for a pair of coupled $\mathbb{Z}_2$ gauge fields, with one $\mathbb{Z}_2$ gauge field living on each cubic lattice. Imposing the above sign structure for the two sets of electric flux lines is equivalent to binding the electric flux line of each gauge field to the magnetic flux line of the other, as will be clear shortly.

It is straightforward to write down a gapped parent Hamiltonian $\mathcal{H}_{\text{linking}}$ for $|\Psi\rangle$, using the fact that flipping the occupancy of all the links on the plaquette changes the linking number $X(\mathcal{C}_A,\mathcal{C}_B)$ if and only if the link piercing the plaquette is occupied. $\mathcal{H}_{\text{linking}}$ is a sum of terms for the plaquettes p of each cubic lattice:

$$\mathcal{H}_{\text{linking}} = -\left(J \sum_{p\in A} \mathcal{F}_{Ap} + J \sum_{p\in B} \mathcal{F}_{Bp} \right). \tag{5}$$

The operators $\mathcal{F}_A$ and $\mathcal{F}_B$ flip the occupancy of the links on a plaquette, with a sign that depends on whether the link piercing it is occupied. Allowing p to denote both a plaquette and the link piercing it and denoting the Pauli operators on A and B by $\vec{\sigma}$ and $\vec{\tau}$, respectively,

$$\mathcal{F}_{Ap} = \tau^z_p \prod_{l\in p} \sigma^x_l, \quad \mathcal{F}_{Bp} = \sigma^z_p \prod_{l\in p} \tau^x_l. \tag{6}$$

These operators all commute, so the Hamiltonian is trivially solvable. $|\Psi\rangle$ is the unique ground state and minimizes each term of $\mathcal{H}_{\text{linking}}$ since $\mathcal{F}\,|\Psi\rangle = |\Psi\rangle$ for each plaquette operator.

The state $|\Psi\rangle$ contains only closed loops; that is, it satisfies

$$\prod_{l\in v} \sigma^z_l = 1 \quad \text{for } v \in A, \qquad \prod_{l\in v} \tau^z_l = 1 \quad \text{for } v \in B, \tag{7}$$

where v denotes a vertex and $l \in v$ denotes the links touching v. Any state satisfying $\mathcal{F}\,|\Psi\rangle = |\Psi\rangle$ for all the plaquette operators must also satisfy these vertex conditions because $\prod_{l\in v} \sigma^z_l$ and $\prod_{l\in v} \tau^z_l$ can be written as products of $\mathcal{F}$s.

We may regard Eqs. (7) as the gauge constraints for a pair of pure $\mathbb{Z}_2$ gauge theories (the $\mathbb{Z}_2$ versions of $\vec{\nabla}\cdot\vec{E} = 0$). The two electric fields are given by σ^z and τ^z and live on the links of A and B, respectively. The magnetic field of each gauge field lives on the links of the *opposite* lattice to its electric field. For example, the magnetic field of σ is given by $\prod_{l\in p} \sigma^x$, where p is a plaquette of A or, equivalently, a link of B.

In this language, $\mathcal{H}_{\text{linking}}$ simply glues the electric flux line of each species to the magnetic flux line of the other. The σ-magnetic flux and the τ-electric flux are equal since $\mathcal{F}_A = 1$, and the σ-electric and τ-magnetic fluxes are equal via $\mathcal{F}_B = 1$.

The state $|\Psi\rangle$ is not topologically ordered. Neither is it a time-reversal-protected SPT: it can be adiabatically transformed to a product state without breaking time-reversal symmetry. However, it *is* protected if we impose Eqs. (7) as constraints, i.e., if we forbid open strands (as opposed to closed loops). In the gauge-theory language, this means forbidding charge. With this constraint it is impossible to reach a trivial state without going through a phase transition, as follows from the self-duality of the state described in Sec. III A.

We will explain these features from several points of view below. One convenient approach which leads to a geometric picture is to switch from the (σ^z,τ^z) basis used in Eq. (4) to the (σ^z,τ^x) basis. The σ^z configuration is a loop configuration on the A lattice, as above. We represent the τ^x configuration by a configuration of *membranes* made up of plaquettes on the A lattice: $\tau^x_p = -1$ represents an occupied plaquette, and $\tau^x_p = 1$ represents an unoccupied one.

The $\mathcal{F}_B$ terms in $\mathcal{H}_{\text{linking}}$ act on a link of the A lattice together with the four plaquettes touching it. $\mathcal{F}_B = 1$ imposes the rule that the σ^z loops are glued to the boundaries of the τ^x membranes, i.e., to the links where an odd number of occupied plaquettes meet. This is the gluing of σ-electric flux lines (where $\sigma^z = -1$) to τ-magnetic flux lines (where $\prod \tau^x = -1$) mentioned above.

Let $\mathcal{M}$ denote a membrane configuration, and let $|\mathcal{M}\rangle$ denote the corresponding state with $\tau^x = -1$ on the occupied plaquettes. Let $\partial\mathcal{M}$ be the loop configuration given by the boundaries of the membranes in $\mathcal{M}$. Then $|\Psi\rangle$ can be written (neglecting an overall constant)

$$|\Psi\rangle = \sum_{\mathcal{C}_A} \sum_{\substack{\mathcal{M} \\ \partial\mathcal{M}=\mathcal{C}_A}} |\mathcal{C}_A\rangle\, |\mathcal{M}\rangle\,. \tag{8}$$

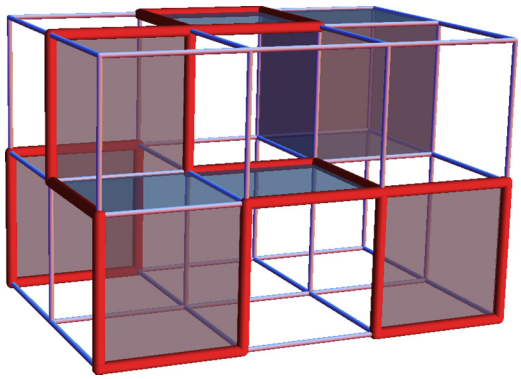

FIG. 4. (Color online) After a basis change, $|\Psi\rangle$ is a superposition of membrane configurations ($\tau^x = -1$ on shaded plaquettes) with red loops (where $\sigma^z = -1$) glued to membrane boundaries. (The red loops are σ-electric lines, and the membrane boundaries are τ-magnetic lines.)

Figure 4 shows the geometrical interpretation of this state. It is a soup of τ^x membranes, with σ^z loops glued to their boundaries.

Confinement of string end points is easy to see in this basis. A pair of vertex excitations at which $\prod_{l\in v}\sigma_l^z = -1$ is connected by an open string. Since the boundary of $\mathcal{M}$ contains only closed loops, the open string makes it impossible to satisfy the gluing of strings to membrane boundaries demanded by the $\mathcal{F}_B$ terms in $\mathcal{H}_{\text{linking}}$. If the separation of the vertex defects is D, there must be at least D unsatisfied links, giving a linear confining potential for such defects. For similar reasons, a configuration with an odd number of winding σ^z strands in some direction costs an energy proportional to the spatial extent of the system in this direction. By symmetry, this applies equally to the τ^z strings that are present in the original basis.

We can also understand the confinement of string end points algebraically (Refs. [11,21] give analogous arguments for bulk confinement and surface topological order in the Walker-Wang models). The Hamiltonian in Eq. (5) is clearly exactly soluble not just for the ground state but for all excited states. An "elementary" excitation is given by a "defect" in some square plaquette, say on the B lattice, with

$$\mathcal{F}_{Bp} = -1, \tag{9}$$

while $\mathcal{F} = +1$ on all other plaquettes of either sublattice. Such a defect plaquette costs energy $2J$. It leads to a violation of the closed-loop vertex constraint for σ^z on the two vertices of the A sublattice connected by the A link that penetrates the defect plaquette. Thus the excitation we have created has two string end points on nearest-neighbor A sites. To move these string end points apart by a distance D we must create $O(D)$ such defect plaquettes. Consequently, the energy cost is also $O(D)$, and we have linear confinement of string end points.

In the gauge theory language, the reason for the absence of deconfined excitations is that the tensionless lines in this state are not lines of pure electric flux, but rather of electric flux together with magnetic flux of the other species. If such lines could end, their end points would be deconfined excitations. But the Hilbert space does not allow for such excitations: a magnetic flux line cannot terminate in the bulk (by virtue of its definition in terms of, e.g., $\prod \tau^x$).

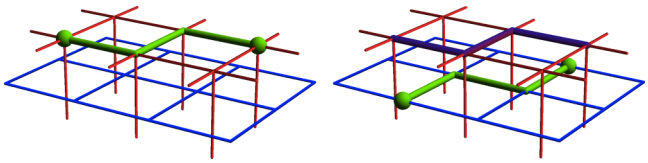

FIG. 5. (Color online) String operators creating surface excitations. (left) Acting with a chain of σ^x operators on the links of the upper layer (A lattice surface) gives a pair of e excitations (i.e., end points of bulk A strings). (right) A pair of m excitations (i.e., end points of B strings) are created by a chain of τ^x operators (thick green strand) on the lower layer (B surface), together with σ^z operators on the corresponding links in the upper layer (thick purple links).

Despite the lack of deconfined end points in the bulk, A and B strings that terminate on a boundary can give deconfined e and m particles in a surface $\mathbb{Z}_2$ topologically ordered state. To see this, we terminate the system as in Fig. 5, including in the Hamiltonian the natural plaquette and vertex terms at the surface. The surface string operators that create pairs of e or pairs of m excitations can then be written explicitly (see Fig. 5). They satisfy the same algebra as the string operators in the toric code [14], confirming that e and m are mutual semions, as expected from the heuristic argument of Fig. 2 .

We can adiabatically transform $|\Psi\rangle$ to a product state as long as we allow the intermediate states to violate the closed-loop constraints on at least one sublattice. The membrane picture gives an obvious way to do this, by giving the membranes in $\mathcal{M}$ a surface tension. If "Area" denotes the number of occupied plaquettes in $\mathcal{M}$, the interpolating state is

$$|\Psi\rangle_\gamma = \sum_{\mathcal{C}_A} \sum_{\substack{\mathcal{M} \\ \partial\mathcal{M}=\mathcal{C}_A}} e^{-\gamma\times\text{Area}}\,|\mathcal{C}_A\rangle\,|\mathcal{M}\rangle\,. \tag{10}$$

When $\gamma = 0$, this is the initial state, and when $\gamma \to \infty$, only the term with zero area survives. This is the state with no loops and no membranes, i.e., the product state $|\sigma^z = 1\rangle|\tau^x = 1\rangle$. To get a gapped parent Hamiltonian for $|\Psi\rangle_\gamma$, we modify the plaquette flip term $\mathcal{F}_A$ in $\mathcal{H}_{\text{linking}}$ to $\mathcal{F}_{Ap} = (\cosh\gamma)^{-1}[\tau_p^z\prod_{l\in p}\sigma_l^x + (\sinh\gamma)\,\tau_p^x]$. This preserves the simple algebraic properties of the plaquette terms. From the fact that the modified $\mathcal{F}_{Ap}$ does not commute with the closed-loop constraint on the B lattice (or by directly transforming to the τ^z basis) we see that $|\Psi\rangle_\gamma$ violates this constraint when $\gamma > 0$.

A. Self-duality of $|\Psi\rangle$ and protection by constraints

When the interpolating state above is rewritten in the original (σ^z,τ^z) basis, it includes configurations with open strands, as well as closed loops, on the B lattice. What if we impose the constraint that both lattices have only closed loops? In this case it is impossible to go from $|\Psi\rangle$ to a trivial state without a phase transition. (We will take the reference trivial state to be that with no loops, $|\text{trivial}\rangle = |\sigma^z = 1\rangle\,|\tau^z = 1\rangle$.)

This follows from a simple duality transformation which exchanges the electric flux of each species with the magnetic flux of the other species. The duality maps $|\Psi\rangle$ to itself but exchanges the trivial state with a topologically ordered one. Thus there is no adiabatic path from $|\Psi\rangle$ to the trivial state.

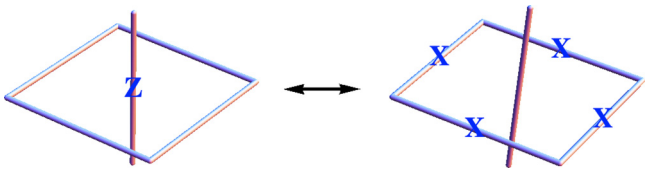

FIG. 6. (Color online) Under the mapping (11), a σ^z (τ^z) operator on a link is exchanged with a product of τ^x (σ^x) operators on the surrounding links of the other lattice. (Links of one lattice can equally be thought of as plaquettes of the other.)

If there were, duality would yield an adiabatic path from $|\Psi\rangle$ to the topologically ordered state, and this is impossible since $|\Psi\rangle$ is not topologically ordered.

The duality transformation makes sense for states obeying the closed-loop constraint. (To be precise, we must also impose the global constraint that the loop configurations have even winding in each direction.) As shown in Fig. 6, its action is

$$\sigma_l^z \longleftrightarrow \prod_{p\in l} \tau_p^x, \quad \tau_p^z \longleftrightarrow \prod_{l\in p} \sigma_l^x. \tag{11}$$

Here $p \in l$ denotes the four plaquettes p surrounding link l. We have labeled the σ's by l for link and the τ's by p for plaquette, but the duality acts on the two sets of degrees of freedom symmetrically. It preserves the locality of any Hamiltonian acting in the constrained Hilbert space.

For completeness, we write the action of the duality on states explicitly. Return to the picture of loops plus membranes on the A lattice, i.e., the (σ^z, τ^x) basis. One may check that any state satisfying the constraints can be written as a sum over two loop configurations on the *same* lattice,

$$|f\rangle = \sum_{\mathcal{C}_A, \mathcal{C}'_A} f(\mathcal{C}_A, \mathcal{C}'_A)\, |\mathcal{C}_A\rangle_\sigma\, |\widetilde{\mathcal{C}'_A}\rangle_\tau, \tag{12}$$

where $|\widetilde{\mathcal{C}'_A}\rangle_\tau$ is defined as the uniform superposition of all membrane configurations $|\mathcal{M}\rangle_\tau$ with boundary $\partial\mathcal{M} = \mathcal{C}'_A$. We have added subscripts to the kets as a reminder of the degrees of freedom involved. ($\mathcal{C}_A$ is the σ-electric flux configuration, and $\mathcal{C}'_A$ is the τ-magnetic flux configuration; the fact that the wave function depends on $\mathcal{M}$ only through $\partial\mathcal{M}$ is simply a statement of gauge invariance.) The duality then simply exchanges the two kinds of loops,

$$f(\mathcal{C}_A, \mathcal{C}'_A) \longleftrightarrow f(\mathcal{C}'_A, \mathcal{C}_A). \tag{13}$$

The flip operators $\mathcal{F}_A$ and $\mathcal{F}_B$ [Eq. (6)] are clearly invariant under the duality in Eq. (11), and therefore so is $\mathcal{H}_{\text{linking}}$. [We can also see that $|\Psi\rangle$ is invariant from Eqs. (13) and (8).] On the other hand, the trivial Hamiltonian

$$\mathcal{H}_{\text{trivial}} = -\left(J \sum_{l\in A} \sigma_l^z + J \sum_{l\in B} \tau_l^z \right) \tag{14}$$

is exchanged with

$$\mathcal{H}_{\text{deconfined}} = -\left(J \sum_{p\in A} \prod_{l\in p} \sigma_l^x - J \sum_{p\in B} \prod_{l\in p} \tau_l^x \right), \tag{15}$$

which describes a pair of deconfined $\mathbb{Z}_2$ gauge theories. This establishes the claim at the beginning of this section: while the linking state is invariant, the trivial state is exchanged with a topologically ordered state. It follows that the linking state is in a distinct phase from the trivial state if we do not allow open end points in the Hilbert space. [We know from Eq. (10) that they are in the same phase if we *do* allow end points.]

B. Heuristic relation between symmetry protection of $eTmT$ and the closed-loop constraint

The proposed wave function for the $eTmT$ phase has the two loop species "stuffed" with Haldane/AKLT chains. The linking sign factor ensures that the ground state is not topologically ordered as required for a topological paramagnet. In particular the open end points of the loops, which now harbor a Kramers doublet, are confined. However, as described in Sec. II A the surface implements time reversal "anomalously" exactly characteristic of the $eTmT$ state.

We now briefly consider whether the results in the previous section for the pure-loop state yield a heuristic "bulk" understanding of why the $eTmT$ state is protected by time reversal. So let us imagine perturbing the schematic $eTmT$ wave function of Sec. II A and ask why we cannot reach a trivial state without a phase transition.

We make use of the heuristic analogy between the AKLT loops of the spin-1 system and the pure loops of the coupled gauge theory [33]. The result for the pure-loop state then indicates that if we have only closed AKLT loops on each sublattice, we cannot get to a trivial state without a phase transition. So we must consider proliferating open strands on at least one sublattice. But in the spin-1 system, unlike the pure-loop system, open strands introduce bulk spin-1/2 Kramers doublet degrees of freedom. (Binding these emergent spin-1/2s into singlets with others on the same sublattice merely heals the AKLT chains, taking us back to the original situation with separate closed loops on each sublattice.) When time reversal is broken, these spin-1/2s are innocuous: for example, we can gap them out using a magnetic field. But it is natural to expect that when time reversal is preserved, they prevent us from reaching a trivial state without closing the gap.

However, the above argument is incomplete as it does not rule out the possibility of getting to a trivial state by proliferating nearby pairs of open strands on *opposite* sublattices. Such a pair gives two spin-1/2s which can be bound into a singlet to avoid a gapless degree of freedom. In the gauge theory, such pairs correspond to bound pairs of electric charges, one from each $\mathbb{Z}_2$ gauge field. The stability of the $eTmT$ state suggests that the pure loop state remains protected even when such double charges are allowed. We note that at the surface these double charges correspond to the bound state of the e and m particles (in the surface topological order). This is a Kramers singlet spin-0 fermion (conventionally denoted ϵ). The surface Fermi statistics suggests a potential obstruction to "trivializing" the bulk by proliferating the double charges. We leave an explicit demonstration of this for the future.

IV. PARTON CONSTRUCTIONS

Although the description of the $eTmT$ topological paramagnet in terms of a loop-gas wave function is physically appealing, it is desirable to have alternate descriptions which enhance

our understanding and which may help with evaluating the energetic stability of this phase in microscopic models. To that end, in this section we propose explicit parton constructions for some topological paramagnets in spin-1 systems.

Historically, the parton approach has provided variational wave functions and effective field theories both for spin liquids [3] and nonfractionalized symmetry-breaking states [34]. The parton construction inevitably introduces a gauge symmetry. It describes a fractionalized spin-liquid phase whenever it yields an emergent deconfined gauge field. To obtain a nonfractionalized phase such as a conventional antiferromagnet or a valence-bond solid paramagnet, the gauge field should either be Higgsed or confined.

Recently, partons have been used to construct SPT states in two [35,36] and three [37,38] dimensions. The general idea is to construct a gauge theory (with matter fields) that is confined, but with certain nontrivial features surviving in the confined state that make it an SPT state. However, the currently known constructions in three dimensions use either $\mathbb{Z}_2$ or U(1) gauge theories, which do not confine automatically: strong gauge coupling is needed to reach the confined phase. Furthermore, the constructions using U(1) gauge theories [37] require highly nontrivial dynamics of the gauge fields to condense composite dyonlike objects.

In three dimensions, a continuous non-Abelian gauge symmetry is needed to guarantee confinement. We propose two parton constructions in three dimensions with SU(2) gauge symmetry, which confine even if the bare gauge coupling is small, giving rise to topological paramagnets. A similar construction was used previously [36] in two dimensions to describe an SPT phase of a spin-1 magnet protected by spin SU(2) symmetry and time reversal. We also propose a construction with U(1) gauge symmetry, which confines at sufficiently strong coupling. Crucially, this U(1) construction differs from previous ones in that we condense only simple monopoles to confine the gauge theory, which can be achieved at strong coupling without exotic form of gauge field dynamics.

The spin-1 operators are rewritten using the two-orbital fermionic parton representation proposed in Ref. [16],

$$\vec{S} = \frac{1}{2}\sum_{a=1,2} f^\dagger_{a\alpha}\vec{\sigma}_{\alpha\beta}f_{a\beta}, \tag{16}$$

where $a = 1,2$ is the orbital index. As will be discussed below, the two-orbital structure is natural for topological bands corresponding to topological paramagnets. This gives another reason for favoring spin-1 systems.

The physical spin states are represented in the parton description as

$$|S_z = 0\rangle = \frac{1}{\sqrt{2}}(f^\dagger_{1\downarrow}f^\dagger_{2\uparrow} + f^\dagger_{1\uparrow}f^\dagger_{2\downarrow})|\text{vac}\rangle,$$
$$|S_z = +1\rangle = f^\dagger_{1\uparrow}f^\dagger_{2\uparrow}|\text{vac}\rangle, \quad |S_z = -1\rangle = f^\dagger_{1\downarrow}f^\dagger_{2\downarrow}|\text{vac}\rangle,$$

where $|\text{vac}\rangle$ is the state with no fermions. States in the physical spin Hilbert space thus have two fermions at each site, $\sum_{a\alpha} f^\dagger_{a\alpha}f_{a\alpha} = 2$, and the two fermions form a singlet in orbital space: denoting the Pauli matrices in orbital space by $\tau^{x,y,z}$, this is $\sum_\alpha f^\dagger_{a\alpha}\vec{\tau}_{ab}f_{b\alpha} = 0$.

The representation in Eq. (16) actually has an Sp(4) gauge redundancy [16] which becomes apparent when we represent the fermions using Majoranas, $f = \frac{1}{2}(\eta_1 - i\eta_2)$. Here $\eta_{1,2}$ are Hermitian operators satisfying $\{\eta_{sI},\eta_{s'J}\} = 2\delta_{ss'}\delta_{IJ}$, where $s,s' = 1,2$ are the new indices associated with the Majoranas and I,J represent all other indices (site, spin, orbital). The Majorana representation of the spin is

$$\vec{S} = \tfrac{1}{8}\eta^T\vec{\Sigma}\,\eta, \quad \vec{\Sigma} = (\rho^y\sigma^x,\sigma^y,\rho^y\sigma^z), \tag{17}$$

where $\rho^{x,y,z}$ are Pauli matrices acting on the Majorana index. The generators of the gauge symmetry are ten antisymmetric imaginary matrices that commute with the physical spin operators:

$$\Gamma = \{\rho^y,\rho^y\tau^{x,z},\rho^{x,z}\sigma^y,\rho^{x,z}\sigma^y\tau^{x,z},\tau^y\}, \tag{18}$$

where τ_i are Pauli matrices acting on the orbital index. The spin in Eq. (17) is invariant under the Sp(4) gauge transformation $\eta \to e^{ia_i\Gamma_i}\eta$.

The effective field theory associated with the parton construction is a gauge theory. The gauge symmetry is determined by the mean-field band structure of the partons and is, in general, a subgroup of the full Sp(4) group due to some generators being Higgsed. The gauge structure allows symmetry to act projectively on the η fermion [3]. In particular, time reversal could be either Kramers ($\mathcal{T}^2 = -1$) or non-Kramers ($\mathcal{T}^2 = 1$).

In three dimensions, band structures of Kramers fermions with $\mathcal{T}$ symmetry are classified by an integer index [39] ν which counts the number of Majorana cones on the surface. It was realized [40–42] that in the presence of interactions the state with $\nu = 16$ is trivial, while that with $\nu = 8$ is equivalent to a topological paramagnet. More specifically, for $\nu = 8$ the surface state with four Dirac cones (eight Majorana cones) can be gapped without breaking any symmetry via strong interactions, and the resulting gapped surface state must have intrinsic topological order. The simplest such topological order is a $\mathbb{Z}_2$ gauge theory in which the e and m particles are bosons but transform under time reversal as Kramers doublets ($\mathcal{T}^2 = -1$). Therefore we can put the slave fermions into a band with $\nu = 8$ and let the gauge fields confine the fermions [either automatically through an SU(2) gauge field or at strong coupling through a U(1) gauge field]. Crucially, the topological quasiparticles (e and m) on the surface do not carry the gauge charge, and they survive on the surface as deconfined objects. The resulting phases are therefore confined paramagnets with nontrivial surface states protected by time-reversal symmetry.

Non-Kramers fermions, by contrast, cannot host nontrivial band structure with time-reversal symmetry alone. However, if spin-S_z conservation is present, the band structures can again be assigned an integer topological invariant ν' [39], which is the number of Dirac cones on the surface (or half the number of Majorana cones). It is known [40–43] that with interactions the state with $\nu' = 8$ is trivial, while that with $\nu' = 4$ is equivalent to a topological paramagnet. We can then put the slave fermions into a band with $\nu' = 4$ and let the gauge fields confine the fermions, which produces a topological paramagnet with time reversal and spin-S_z conservation.

In both cases we need to put the slave fermions into band structures with four Dirac cones on the surface. Band

structures with two Dirac cones ($\nu = 4$) have been studied on the cubic [44] and diamond [45] lattices. Therefore we can obtain the desired structure simply by putting the partons into two copies of the $\nu = 4$ band. This can be easily done by taking advantage of the two orbitals in Eq. (16), making the topological paramagnets very natural in spin-1 systems.

In the next section we outline a similar construction for the one-dimensional Haldane chain by confining slave fermions which form four copies of the Kitaev chain. This illustrates the essential idea of our constructions in a simpler and more familiar context.

A. Parton construction for Haldane/AKLT chain

The Haldane phase is an SPT phase with gapless boundary degrees of freedom that are protected by time reversal. As a warm-up exercise, we outline how this phase can be constructed from a topological superconductor of slave fermions. This illustrates some features we will meet again in three dimensions. A different parton construction for the Haldane phase was considered in Ref. [46].

The fermions are taken to be non-Kramers ($\mathcal{T}^2 = 1$). In one dimension, superconducting band structures for *free* non-Kramers fermions are labeled by a $\mathbb{Z}$-valued index [39], ν, which is the number of protected Majorana zero modes at the boundary. The state with a given ν can be viewed as ν copies of Kitaev's p-wave superconducting chain [47]. Interactions reduce this classification to $\mathbb{Z}_8$; that is, the $\nu = 8$ state becomes trivial [6]. Further, the state with $\nu = 4$ is topologically equivalent to the Haldane chain, modulo the presence of gapped fermions in a trivial band.

Here we therefore put the slave fermions into four copies of the Kitaev band structure, in an SU(2)-symmetric manner. Gauge fluctuations (or Gutzwiller projection) will then remove the unwanted degrees of freedom, leaving a topological paramagnet in the Haldane phase.

Starting with an antiferromagnetic spin-1 chain,

$$\mathcal{H} = J \sum_i \vec{S}_i \cdot \vec{S}_{i+1} + \cdots , \tag{19}$$

we represent the spins with slave fermions as in Eq. (16) or, equivalently, Eq. (17). The valence-bond picture of the AKLT state suggests using a mean-field Hamiltonian for the partons with hopping t and spin-singlet, orbital-singlet pairing Δ,

$$H_{\mathrm{MF}} = -\sum_i [t(f_i^\dagger f_{i+1} + \mathrm{H.c.}) + \Delta(f_i^\dagger \sigma^y \tau^y f_{i+1}^{\dagger T} + \mathrm{H.c.})].$$

In terms of the Majoranas, this is

$$H_{\mathrm{MF}} = -\frac{1}{2}\sum_i \eta_i^T M \eta_{i+1}, \quad M = t\rho^y + i\Delta\rho^x\sigma^y\tau^y. \tag{20}$$

We first consider this as a free-fermion problem, then include the gauge fluctuations.

For simplicity take $\Delta = t$, which makes the terms in H_{MF} for different links commute. The Hamiltonian is simply four copies of the Kitaev chain, as can be seen immediately by going to a basis where $\sigma^y\tau^y$ is diagonal. To be more explicit, it is useful to define the matrix

$$X = \rho^z\sigma^y\tau^y. \tag{21}$$

First, we use this to define the action of time reversal $\mathcal{T}$ on the fermions:

$$\mathcal{T} : \eta \longrightarrow X\eta. \tag{22}$$

This definition ensures that the spin changes sign under $\mathcal{T}$ and that H_{MF} is invariant. The fermions are non-Kramers ($\mathcal{T}^2 = 1$ on η).

Second, let us define matrices that project onto a given value of X and corresponding fermion modes:

$$\mathcal{P}_\pm = \tfrac{1}{2}(1 \pm X), \quad \eta^{(\pm)} = \mathcal{P}_\pm \eta. \tag{23}$$

In an appropriate basis, $\eta^{(+)}$ has four nonzero components. Next, note that

$$M = \mathcal{P}_- M \mathcal{P}_+ \tag{24}$$

since $M = t\rho^y(1 + \rho^z\sigma^y\tau^y) = (2t\rho^y)\mathcal{P}_+$ and so on. So we may rewrite H_{MF} as

$$H_{\mathrm{MF}} = -\frac{1}{2}\sum_i \eta_i^{(-)T} M \eta_{i+1}^{(+)}. \tag{25}$$

Taking open boundary conditions and denoting the leftmost site of the chain by L, we see that the four modes in $\eta_L^{(+)}$ do not appear in the Hamiltonian.

These four Majoranas correspond to two complex fermion modes that can be occupied or unoccupied, i.e., to a degenerate four-dimensional boundary Hilbert space. At the level of free fermions, this degeneracy is protected by time-reversal symmetry $\mathcal{T}$, under which $\eta_L^{(+)}$ is invariant (since by definition $X\eta^{(+)} = \eta^{(+)}$) [48].

Once we go beyond mean-field theory, the fermions are coupled to confining gauge fluctuations. We will see below that two of the four boundary states are not gauge invariant; that is, they can be thought of as having an unscreened gauge charge sitting at the end of the chain. Confinement removes these states from the low-energy Hilbert space, leaving a single-boundary spin-1/2 whose gaplessness is protected by time reversal.

H_{MF} treats spin and orbital degrees of freedom symmetrically and preserves $\mathrm{SU(2)_{spin}} \times \mathrm{SU(2)_{orbital}}$ symmetry. The four boundary states can be labeled by the occupation numbers of two complex fermions $c_{1,2}$. Since the partons transform as doublets under each SU(2), the fermions $c_{1,2}$ should also form doublets under each SU(2). In an appropriate basis the transformations are

$$\begin{aligned} &\mathrm{SU(2)_{spin}} : (c_1, c_2)^T \longrightarrow \mathcal{U}_s (c_1, c_2)^T, \\ &\mathrm{SU(2)_{orbital}} : (c_1, c_2^\dagger)^T \longrightarrow \mathcal{U}_o (c_1, c_2^\dagger)^T, \end{aligned} \tag{26}$$

where $\mathcal{U}_{s,o}$ are SU(2) matrices. It follows that states which are singlets under $\mathrm{SU(2)_{spin}}$ are doublets under $\mathrm{SU(2)_{orbital}}$ and vice versa. We denote the spin doublet $|\uparrow\rangle, |\downarrow\rangle$ and the orbital doublet $|1\rangle, |2\rangle$. The spin operator for the boundary spin-1 can be split into contributions from the dangling boundary modes $\eta_L^{(+)}$ and from $\eta_L^{(-)}$: $\vec{S}_L = \vec{S}_L^{(+)} + \vec{S}_L^{(-)}$, with

$$\vec{S}^{(\pm)} = \tfrac{1}{8}\eta^{(\pm)T}\vec{\Sigma}\,\eta^{(\pm)}, \quad \vec{\Sigma} = (\rho^y\sigma^x, \sigma^y, \rho^y\sigma^z). \tag{27}$$

We can make a similar splitting for the orbital spin $\vec{T}$, which is related to $\vec{S}$ by swapping the σ's for τ's. We denote the

matrices appearing in $\vec{T}$ by $\vec{\Omega}$:

$$\vec{T}^{(\pm)} = \tfrac{1}{8}\eta^{(\pm)T}\vec{\Omega}\,\eta^{(\pm)}, \quad \vec{\Omega} = (\rho^y\tau^x, \tau^y, \rho^y\tau^z). \tag{28}$$

The pairs $(|\uparrow\rangle, |\downarrow\rangle)$ and $(|1\rangle, |2\rangle)$ are both Kramers doublets since the spin and orbital operators for the boundary modes, $\vec{S}_L^{(+)}$ and $\vec{T}_L^{(+)}$, change sign under $\mathcal{T}$. This can also be checked explicitly by considering the transformation of the boundary states (labeled by fermion occupation numbers) under $\mathcal{T}$, with the fermions transforming as $\mathcal{T} : c_{1,2} \to c_{1,2}^\dagger$.

Now we consider the effect of gauge fluctuations or Gutzwiller projection. We have listed the generators for the Sp(4) gauge group in Eq. (18). However, some gauge generators are Higgsed in the above mean-field state. In general, to determine the unbroken gauge group we must examine Wilson loops of the form $W = \hat{u}_{i_1 i_2}\hat{u}_{i_2 i_3}\cdots\hat{u}_{i_n i_1}$, where $H_{\rm MF} = \sum_{ij}\eta_i^T\hat{u}_{ij}\eta_j$ [3]. The unbroken gauge generators are those that commute with the Wilson loops. Here the only nontrivial Wilson loop is the matrix X defined in Eq. (21). This leaves a subset of six unbroken generators, which may be written in terms of the matrices Ω appearing in the orbital spin [Eq. (28)]:

$$\Gamma_{\rm 1D} = \{\vec{\Omega}, X\vec{\Omega}\}. \tag{29}$$

Taking linear combinations, we can use instead [49]

$$\Gamma_{\rm 1D} = \{\mathcal{P}_+\vec{\Omega}\mathcal{P}_+, \mathcal{P}_-\vec{\Omega}\mathcal{P}_-\}. \tag{30}$$

We denote the unbroken gauge group $\mathrm{SU}(2)^{(+)}_{\rm orbital} \times \mathrm{SU}(2)^{(-)}_{\rm orbital}$.

To make the Hamiltonian in Eq. (20) a reasonable ansatz, we must check that the Sp(4) gauge charges are all zero on average: $\langle\Gamma_i\rangle = 0$ for all i. Fortunately, the unbroken gauge symmetry $\Gamma_{\rm 1D}$ guarantees this.

The boundary modes involve only $\eta^{(+)}$, so they are invariant under $\mathrm{SU}(2)^{(-)}_{\rm orbital}$. However, $|1\rangle$ and $|2\rangle$ are not invariant under $\mathrm{SU}(2)^{(+)}_{\rm orbital}$. Therefore after confinement only the doublet $|\uparrow\rangle, |\downarrow\rangle$ survives, with corresponding spin $\vec{S}_L^{(+)}$. This is the boundary spin-1/2 of the Haldane phase.

In this 1D example we can confirm explicitly that Gutzwiller projecting the mean-field wave function gives the desired SPT phase. In fact the Gutzwiller-projected state for $\Delta = t$, denoted $|\Psi_{\rm spin}\rangle$, is precisely the AKLT state. To see this we adopt a trick from Ref. [46]. Using the fact that the terms in $H_{\rm MF}$ commute, we can check that $|\Psi_{\rm spin}\rangle$ has zero amplitude for a pair of adjacent sites to be in a spin-2 state. $|\Psi_{\rm spin}\rangle$ is therefore the ground state of the AKLT Hamiltonian since this can be written as a sum of projectors onto the spin-2 subspace for each link [50].

It is interesting to consider inversion symmetry here. In the free-fermion problem, $\nu \to -\nu$ under inversion, so that a nonzero value of ν can be realized only with a Hamiltonian which breaks inversion symmetry. With interactions, $\nu \simeq \nu + 8$, suggesting that $\nu = 4$ can be realized in inversion-symmetric interacting system [51]. The present example is a nice realization of this. The mean-field Hamiltonian $H_{\rm MF}$ appears to break inversion symmetry. However, the symmetry can be restored by combining it with a gauge rotation. So the projected wave function is actually inversion symmetric.

We now move on to 3D states.

B. Cubic lattice

Making use of the cubic band structure studied in Ref. [44], we construct an SU(2) gauge theory which confines to a topological paramagnet. We choose the mean-field Hamiltonian

$$H_{\rm MF} = \sum_{\langle ij\rangle} t_{ij}\eta_i^T\rho^y\eta_j + \sum_{\langle\langle ij\rangle\rangle} i\chi'_{ij}\eta_i^T\rho^x\sigma^y\tau^y\eta_j + \sum_{\langle\langle\langle ij\rangle\rangle\rangle} \chi_{ij}\eta_i^T\rho^x\sigma^y\eta_j, \tag{31}$$

where the nearest-neighbor hopping t_{ij} gives a π flux on every square plaquette, the body-diagonal pairing χ_{ij} follows the pattern studied in Ref. [44], and the next-nearest-neighbor pairing χ'_{ij} is a small perturbation introduced to reduce the gauge group to SU(2) and is not responsible for the gap or the band topology.

To determine the unbroken gauge group, we examine the Wilson loops as above. The fundamental nontrivial ones are proportional to $\rho^z\sigma^y$ and $\rho^x\sigma^y\tau^y$. The unbroken gauge group is generated by those of the Sp(4) generators that commute with the Wilson loops. It is then straightforward to see that the unbroken gauge group is an SU(2) generated by

$$\Gamma_{\rm cubic} = \{\rho^z\sigma^y\tau^x, \tau^y, \rho^z\sigma^y\tau^z\}. \tag{32}$$

One can choose to implement time reversal $\mathcal{T}$ as $\mathcal{T} : \eta \to i\rho^z\sigma^y\eta$, and it is straightforward to see that $\mathcal{T} : H_{\rm MF} \to H_{\rm MF}, \vec{S} \to -\vec{S}$ and $\vec{\Gamma}_{\rm cubic} \to -\vec{\Gamma}_{\rm cubic}$. The band structure in Eq. (31) preserves time-reversal symmetry, and the SU(2) gauge rotation commutes with $\mathcal{T}$. Notice also that $\mathcal{T}^2 = -1$ on the η fermions.

We must check that the Sp(4) gauge charges are all zero on average, $\langle\Gamma_i\rangle = 0$. The unbroken gauge symmetry $\Gamma_{\rm cubic}$ guarantees that $\langle\Gamma_i\rangle = 0$ for all i except for $\Gamma_5 = \rho^z\sigma^y$. Furthermore, time-reversal invariance $\mathcal{T}$ guarantees that $\langle\Gamma_5\rangle = 0$. Hence the condition is, indeed, satisfied for any i.

To determine the band topology, it is sufficient to consider the Hamiltonian $H'_{\rm MF}$ with only the nearest-neighbor and body-diagonal terms in Eq. (31). In $H'_{\rm MF}$, fermions with different orbital indices are decoupled and form two identical bands. Each band is the same as that studied in Ref. [44], with $\nu = 4$ (two Dirac cones on the surface). So the band has $\nu = 8$ in total (four Dirac cones). So Eq. (31) indeed gives rise to a topological paramagnet.

In order to understand the role played by spin-rotation symmetry, we examine the surface state in more detail. We start from the surface Dirac theory with $\mathrm{SU}(2)_{\rm gauge} \times \mathrm{SU}(2)_{\rm spin} \times \mathcal{T}$ symmetry, with four Dirac cones in total:

$$H = \psi^\dagger(p_x\mu_x + p_y\mu_z)\otimes\tau_0\otimes\sigma_0\psi, \tag{33}$$

with time reversal

$$\mathcal{T} : \psi \to i\mu_y\otimes\tau_0\otimes\sigma_0\psi^\dagger, \tag{34}$$

gauge SU(2)

$$\mathcal{U}_g : \psi \to \mu_0\otimes\mathcal{U}_g\otimes\sigma_0\psi, \tag{35}$$

and spin SU(2)

$$\mathcal{U}_s : \psi \to \mu_0\otimes\tau_0\otimes\mathcal{U}_s\psi. \tag{36}$$

We have denoted the $SU(2)_{gauge}$ Pauli matrices by $\vec{\tau}$, but they should not be confused with the Pauli matrices for the orbital spin.

Next, we will consider driving this surface theory into a $\mathbb{Z}_2$ topologically ordered state by first introducing an order parameter Δ which gaps out the Dirac fermions but breaks time-reversal symmetry and then restoring time-reversal symmetry by proliferating double vortices in Δ. The single vortex remains gapped and gives rise to anyonic surface excitations with nontrivial time-reversal properties.

To analyze the symmetry properties it is useful to consider the auxiliary $U(1)_a$ transformation

$$U_a(\theta) : \psi \to e^{i\theta}\psi \tag{37}$$

[which is an emergent symmetry of Eq. (33) but not a microscopic symmetry]. The gap term of interest is

$$H_\Delta = i\Delta\, \psi \mu_y \otimes \tau_y \otimes \sigma_y \psi + \text{H.c.} \tag{38}$$

This is invariant under the $SU(2)_{gauge} \times SU(2)_{spin}$ symmetry. It is not invariant under time reversal $\mathcal{T}$ or under $U(1)_a$ separately, but it is invariant under the modified time-reversal transformation $\tilde{\mathcal{T}} \equiv U_a(\pi/2)\mathcal{T}$. Notice that $\tilde{\mathcal{T}}^2 = 1$ on the parton fermions ψ, in contrast to the original $\mathcal{T}$ under which they are Kramers.

As shown in Refs. [13,41,42], the fundamental vortex in Δ transforms projectively under $\tilde{\mathcal{T}}$, i.e., $\tilde{\mathcal{T}}^2 = -1$. We now examine the $SU(2)_{gauge} \times SU(2)_{spin}$ spins carried by the vortex. A key point is that there are four Majorana zero modes trapped in the vortex core. One can label the internal Hilbert space with two complex fermions $c_{1,2}$. Since both SU(2) groups are preserved in the intermediate gapped phase and the partons transform as doublets under both SU(2), the two complex fermions $c_{1,2}$ should also be doublets under both SU(2). In an appropriate basis the transformations are

$$\begin{aligned} \mathcal{U}_g &: \ (c_1, c_2)^T \to \mathcal{U}_g (c_1, c_2)^T, \\ \mathcal{U}_s &: \ (c_1, c_2^\dagger)^T \to \mathcal{U}_s (c_1, c_2^\dagger)^T. \end{aligned} \tag{39}$$

It follows that states which are singlets under $SU(2)_{gauge}$ are doublets under $SU(2)_{spin}$ and vice versa. Specifically, there are two distinct kinds of vortices, labeled by the fermion parity $(-1)^{c_1^\dagger c_1 + c_2^\dagger c_2}$: both have $\tilde{\mathcal{T}}^2 = -1$, but one transforms as $(0,1/2)$ under $SU(2)_{gauge} \times SU(2)_{spin}$, and the other transforms as $(1/2,0)$.

We now restore time-reversal symmetry by condensing double vortices that transform trivially under both $SU(2)_{gauge} \times SU(2)_{spin}$ and $\tilde{\mathcal{T}}$, giving $\mathbb{Z}_2$ topological order on the surface [52,53]. Single vortices with even and odd fermion parity yield mutual semions which we denote e and $\tilde{m}$, respectively. Both are Kramers bosons ($\mathcal{T}^2 = -1$), and e transforms as $(0,1/2)$ under $SU(2)_{gauge} \times SU(2)_{spin}$, while $\tilde{m}$ transforms as $(1/2,0)$. Their bound state $\tilde{\epsilon}$ is non-Kramers and fermionic and transforms as $(1/2,1/2)$.

So far, our treatment of the surface has neglected the confining gauge field [54]. When we take it into account, only excitations that are neutral under $SU(2)_{gauge}$ survive. In addition to e, these include bound states $m = \psi\tilde{\epsilon}$ and $\epsilon = \psi\tilde{m}$ got by attaching a ψ fermion to $\tilde{m}$ and $\tilde{\epsilon}$. This shifts the self-statistics, so m is bosonic, while ϵ is fermionic (all three particles are mutual semions). Since ϵ is the bound state of e and m (and its properties follow from this), we do not discuss it further. Note that $m = \psi\tilde{\epsilon}$ is Kramers since ψ is.

The upshot is that the surface topological order surviving after "gauge neutralization" has an e particle that is Kramers and spin doublet and an m particle that is Kramers but spin singlet. Since both e and m are Kramers bosons, this state is, indeed, the $eTmT$ phase, like the wave function discussed in Sec. II.

However, if spin-rotation symmetry is preserved, a finer classification is possible, under which the present state is dubbed $eCTmT$, where C indicates that e is a spin doublet [10,55]. This finer classification emphasizes a difference between the $eTmT$ state constructed here, in which e is a spin doublet and m is not, and that constructed in Sec. II, where both e and m are spin doublets.

Like the 1D example in the previous section, the cubic lattice construction violates inversion symmetry at the free-fermion level (this is inevitable if ν is nontrivial [56]), but the resulting spin state is inversion symmetric as a result of gauge invariance. Here the hopping term in H_{MF} is invariant under inversion, while for an appropriate choice of χ' the pairing terms change sign under inversion. Therefore inversion can be restored by combining it with the gauge transformation $f \to if$, i.e., $\eta \to i\rho^y\eta$. (With the arrow conventions of Sec. II B, the fluctuating AKLT state is also inversion symmetric.)

C. Diamond lattice

Next, we consider parton theories on the diamond lattice, making use of the band structure of Ref. [45]. First, we construct a theory with an SU(2) gauge field which naturally confines (Sec. IV C 1). The resulting state is a topological paramagnet which requires both time-reversal and XY-spin-rotation symmetry to be protected. Then in Sec. IV C 2 we construct a U(1) gauge theory, which confines at strong coupling. The confined state is a topological paramagnet which only requires time-reversal symmetry.

1. *Topological XY paramagnet from SU(2) gauge theory*

The mean-field Hamiltonian is

$$H_{MF} = \sum_{\langle ij\rangle} t\eta_i^T \rho^y \eta_j + \sum_{\langle\langle ij\rangle\rangle} t'_{ij} \eta_i^T \rho^y \eta_j + \sum_{\langle\langle ij\rangle\rangle} \Delta_{ij} \eta_i^T \rho^x \tau^y \eta_j, \tag{40}$$

where the nearest-neighbor hopping t is isotropic, while the next-nearest-neighbor hopping t'_{ij} and pairing Δ_{ij} follow the patterns discussed in Ref. [45]. Notice that the pairing term is a singlet in orbital space but is a triplet in spin space. Hence the spin-rotation symmetry is reduced from SO(3) down to O(2) rotations about the S_y axis, corresponding to XY anisotropy in the spin model.

We again calculate the nontrivial Wilson loops: the simplest nontrivial ones consist of three links and are proportional to ρ^y and $\rho^x\tau^y$. The unbroken gauge group is generated by

$$\Gamma_{\text{diamond}} = \{\rho^y\tau^x, \tau^y, \rho^y\tau^z\}. \tag{41}$$

These are precisely the orbital SU(2) generators $\vec{\Omega}$.

One can implement time-reversal symmetry $\mathcal{T}$ as $\eta \to \rho^z\sigma^y\tau^y\eta$, under which η is non-Kramers ($\mathcal{T}^2 = 1$) and $\vec{S} \to -\vec{S}$ and, of course, $H_{MF} \to H_{MF}$.

As above we must check that the Sp(4) gauge charges are all zero on average: $\langle \Gamma_i \rangle = 0$. The unbroken gauge symmetry Γ_{diamond} guarantees that $\langle \Gamma_i \rangle = 0$ for all i except for $\Gamma_1 = \rho^y$, which is nothing but the total fermion occupation number (minus 2). Fortunately, the mean-field Hamiltonian (40) has a special lattice symmetry [57] that sets $\langle \Gamma_1 \rangle = 0$.

To determine the topology of the mean-field band structure, it is convenient to consider the modified time-reversal symmetry $\mathcal{T}' : \eta \to i\rho^z\tau^y\eta$ (with $\mathcal{T}'^2 = -1$), which is the combination of time reversal and spin rotation $i\sigma_y$. Fermions with different physical spins ($\eta_\uparrow$ and $\eta_\downarrow$) do not mix under the modified time reversal. Furthermore, they are decoupled in the mean-field Hamiltonian H_{MF} and form two copies of an identical band. Therefore the topological index ν' is defined for each band separately. Now each band is identical to that studied in Ref. [45], with $\nu' = 4$. The total band therefore has $\nu' = 8$, with four Dirac cones in total on the surface.

We now consider the surface Dirac theory with $\text{SU}(2)_{\text{gauge}} \times \text{U}(1)_{\text{spin}} \times \mathcal{T}$ symmetry, with four Dirac cones in total:

$$H = \psi^\dagger(p_x\mu_x + p_y\mu_z) \otimes \tau_0 \otimes \sigma_0\psi, \tag{42}$$

with modified time reversal

$$\mathcal{T}' : \psi \to i\mu_y \otimes \tau_0 \otimes \sigma_0\psi^\dagger, \tag{43}$$

gauge SU(2)

$$\mathcal{U}_g : \psi \to \mu_0 \otimes \mathcal{U}_g \otimes \sigma_0\psi, \tag{44}$$

and spin U(1)

$$U_s(\theta) : \psi \to e^{i\theta}\psi. \tag{45}$$

The actual time reversal is $\mathcal{T} = U_s(\pi/2)\mathcal{T}'$:

$$\mathcal{T} : \psi \to \mu_y \otimes \tau_0 \otimes \sigma_0\psi^\dagger. \tag{46}$$

Now, consider the gap term

$$H_\Delta = i\Delta\,\psi\mu_y \otimes \tau_y \otimes \sigma_y\psi + \text{H.c.}, \tag{47}$$

which preserves both $\text{SU}(2)_{\text{gauge}}$ and $\mathcal{T}$ but breaks $\text{U}(1)_{\text{spin}}$. To restore the $\text{U}(1)_{\text{spin}}$ symmetry and preserve the gap, we need to proliferate vortices in the order parameter field Δ. It was shown in Refs. [13,41,42] that the fundamental vortices have $\mathcal{T}^2 = -1$, so condensing double vortices gives a $\mathbb{Z}_2$ gauge theory, with e being Kramers, $\tilde{m}$ being Kramers and $\text{SU}(2)_{\text{gauge}}$ doublet, and $\tilde{\epsilon}$ being non-Kramers and $\text{SU}(2)_{\text{gauge}}$ doublet. We can then gauge neutralize the particles by binding ψ fermions to $\tilde{m}$ and $\tilde{\epsilon}$. The neutralized theory then has e being Kramers and $m = \tilde{\epsilon}\psi$ being non-Kramers (recall that $\mathcal{T}^2 = 1$ on ψ) but carrying spin-1/2 under $\text{U}(1)_{\text{spin}}$ due to the S_y spin carried by ψ. This state is dubbed $eCmT$ in Ref. [10].

The fermions will be confined once the fluctuation of the SU(2) gauge field is introduced, and we obtain a nonfractionalized bulk state. On the surface, the $eCmT$ topological order survives the confinement since all the nontrivial quasiparticles in the theory are gauge neutral and are hence decoupled from the gauge field. We have thus obtained the $eCmT$ topological paramagnet.

As a side note, if the spin-1 operators are pseudospins such that $\mathcal{T} : \{S_x, S_y, S_z\} \to \{S_x, -S_y, S_z\}$, then the modified time reversal $\mathcal{T}' : \eta \to i\rho^z\tau^y\eta$ (with $\mathcal{T}'^2 = -1$) could represent the physical time-reversal symmetry. In this case we obtain a topological paramagnet that requires only time reversal, as will be shown in Sec IV C 2.

2. *Stable U(1) quantum spin liquids and topological paramagnets*

The parton construction, of course, also gives access to stable quantum spin-liquid phases. Of particular interest to us is a time-reversal-symmetric U(1) quantum spin-liquid phase on the diamond lattice. For greater generality we allow for full SU(2) spin symmetry. As usual such a phase has a gapless emergent photon. In addition it has a gapped fermionic spin-1/2 Kramers doublet spinon which has internal "electric" charge [58] and a gapped bosonic spin-0 magnetic monopole that transforms to an antimonopole under time reversal. We will give the spinons the band structure of a topological superconductor (as in previous sections). The resulting quantum spin-liquid phase then inherits the nontrivial surface states of the topological superconductor. The relevance to the present paper comes from asking about the confined phase that results when the magnetic monopole is condensed. We show below that this is the $eCTmT$ topological paramagnet.

SPT phases in three dimensions have been accessed previously through confinement of emergent U(1) gauge fields [37]. However, in these previous studies the confinement was achieved in a highly nontrivial way involving the condensation of dyons (bound states of magnetic and electric charges). The novel aspect of our construction is that the confinement is achieved directly by simply condensing the magnetic monopole, which will result from the usual dynamics of the gauge field at strong coupling.

Consider the following mean-field ansatz:

$$H_{\text{MF}} = \sum_{\langle ij\rangle} t\eta_i^T\rho^y\eta_j + \sum_{\langle\langle ij\rangle\rangle} t'_{ij}\eta_i^T\rho^y\eta_j + \sum_{\langle\langle ij\rangle\rangle} \Delta_{ij}\eta_i^T\rho^x\sigma^y\eta_j + \sum_i \Delta'\eta_i^T\rho^x\sigma^y\eta_i + \sum_{\langle ij\rangle,\, i\in A} it''\eta_i^T\rho^y\tau^y\eta_j, \tag{48}$$

where the nearest-neighbor hopping t and on-site pairing Δ' are uniform and isotropic, while the next-nearest-neighbor hopping t'_{ij} and pairing Δ_{ij} follow the patterns discussed in Ref. [45]. Note that the first two terms are the same as in Eq. (40), and the third is obtained by exchanging the role of orbital and physical spin. Contrary to Eq. (40), the pairing term Δ is a singlet in physical spin and a triplet in orbital space, so the full spin-rotation symmetry is preserved. The nearest-neighbor antisymmetric hopping term t'' is introduced to reduce the gauge symmetry and does not affect the other arguments in this section as long as it is kept small.

The simplest nontrivial Wilson loops are proportional to ρ^y, $\rho^x\sigma^y$, and $\rho^y\tau^y$. The resulting unbroken gauge group is a U(1) generated by τ^y.

We implement time-reversal symmetry $\mathcal{T}$ through $\eta \to i\rho^z\sigma^y\eta$ (which has $\mathcal{T}^2 = -1$). It is straightforward to check that $\vec{S} \to -\vec{S}$ and $H_{\text{MF}} \to H_{\text{MF}}$ under the chosen time-reversal symmetry. Moreover, the U(1) gauge charge τ^y is also odd under $\mathcal{T}$, which allows for topologically nontrivial band structures for the partons.

We now check that $\langle \Gamma_i \rangle = 0$. The unbroken U(1) gauge symmetry and time reversal guarantee that $\langle \Gamma_i \rangle = 0$ for all

i except for ρ^y and $\rho^x\sigma^y$, which are nothing but the total fermion occupation number (minus 2) and the real part of the on-site pairing. The lattice symmetry [57] again sets $\langle\rho^y\rangle = 0$. For the on-site pairing amplitude, there is no symmetry to set it to zero automatically. We must therefore adjust the on-site pairing term Δ' in Eq. (48) to make it zero on average [59].

To determine the topology of the mean-field band structure, notice that fermions with different orbital indices (τ indices) do not mix under time reversal $\mathcal{T} : \eta \to i\rho^z\sigma^y\eta$. They are also decoupled in the mean-field Hamiltonian $H_{\rm MF}$, forming two copies of an identical band. Therefore the topological index ν' is defined for each band separately. Now each band is almost identical to that studied in Ref. [45], with $\nu' = 4$. The total band therefore has $\nu' = 8$, with four Dirac cones in total on the surface.

We now consider fluctuations of the U(1) gauge field. In the weak-coupling regime the gauge theory is deconfined, and we have a stable U(1) quantum spin-liquid phase. The spinon band structure has time-reversal-protected surface states that provide a distinction between this spin liquid and more conventional ones. For a compact U(1) gauge theory, there are always gapped magnetic monopole excitations in the theory. In Refs. [13,41] it was shown that for the spinon band structure we have here, this magnetic monopole is a spin-0 boson that simply transforms into an antimonopole under time reversal.

As the gauge coupling strength increases, the monopole mass gap decreases and eventually becomes zero. The monopoles will then condense and confine the gauge theory. The trivial symmetry properties of the monopole imply that this condensate does not break $\mathcal{T}$ or the physical spin SU(2) (if present). The confined state is thus a nonfractionalized symmetry-preserving paramagnet. To determine which SPT phase the paramagnet belongs to, we need to examine the surface state in more detail. The argument is largely parallel to that in Sec. IV B, with the simple modification that the SU(2) gauge symmetry discussed in Sec. IV B is reduced to U(1). The conclusion remains the same: the paramagnet is the nontrivial SPT dubbed $eCTmT$ in Ref. [10]. The representative surface state is a gapped $\mathbb{Z}_2$ topological order, with e being Kramers and spin-doublet and m Kramers but spin singlet. (If the spin-rotation symmetry is broken, this becomes a generic $eTmT$ state.)

D. Spin wave functions

The parton constructions suggest spin wave functions that may be useful as variational states in future work on specific microscopic models. Following the standard procedure [3], we construct a spin wave function from the mean-field fermion wave function $|\Psi_{\rm MF}\rangle$ by projecting onto the subspace obeying the constraints $\sum_{a\alpha} f^\dagger_{a\alpha} f_{a\alpha} = 2$ and $\sum_{ab\alpha} f^\dagger_{a\alpha}\vec{\tau}_{ab} f_{b\alpha} = 0$:

$$|\Psi_{\rm spin}\rangle = \mathcal{P}|\Psi_{\rm MF}\rangle. \tag{49}$$

Such a projection is expected to roughly mimic the effect of gauge fluctuations. For the states constructed in Secs. IV B and IV C 1, the SU(2) gauge fluctuations automatically confine the states. We therefore expect the projected wave functions to represent the confined spin SPT states. For the state in Sec. IV C 2, the U(1) gauge field is deconfined at weak coupling and confines to an SPT state at strong coupling. So it is not clear *a priori* whether the projected wave function will give the $U(1)$ quantum spin-liquid state or the confined SPT state.

These spin wave functions are alternate possibilities to the loop-gas wave functions described in the first part of the paper. While the loop-gas wave functions are physically appealing, they are likely not very tractable numerically due to the linking signs. The parton wave functions, on the other hand, may be studied through variational Monte Carlo calculations, although the physical connection to SPT physics is less directly obvious. This situation is similar to existing descriptions of quantum spin-liquid phases through either loop gases (string nets) or through partons, which each have their advantages and disadvantages.

For the topological paramagnets, at present we do not have a direct connection between the parton and loop-gas wave functions. Establishing such a connection is a target for future work and will confirm the general correctness of the projected wave functions as faithfully capturing the state accessed through the parton description.

V. DISCUSSION: TOWARD MODELS AND MATERIALS

We have emphasized that frustrated spin-1 magnets in three dimensions may be fruitful in the search for spin SPT phases.

In the ongoing search for quantum paramagnetism in frustrated systems, the bulk of the attention has been focused on spin-1/2 systems. This is guided by the intuition that increasing the spin only leads to more "classical" physics and hence to a greater tendency to order. Caution, however, is required in taking this intuition too seriously. In one dimension the spin-1/2 chain is almost antiferromagnetically ordered (power-law correlations), while the spin-1 chain is a good paramagnet with a spin gap. This has the following amusing consequence. Consider a two-dimensional rectangular lattice with nearest-neighbor antiferromagnetic interactions:

$$H_{\rm rect} = J_\parallel \sum_{\mathbf{r}} \vec{S}_{\mathbf{r}} \cdot \vec{S}_{\mathbf{r}+\mathbf{x}} + J_\perp \sum_{\mathbf{r}} \vec{S}_{\mathbf{r}} \cdot \vec{S}_{\mathbf{r}+\mathbf{y}}. \tag{50}$$

For $J_\parallel = J_\perp$ the model is antiferromagnetically ordered for all spin S. When $\frac{J_\perp}{J_\parallel}$ is decreased from 1, the spin-1/2 model stays ordered unless $J_\perp = 0$. The spin-1 model, on the other hand, becomes a spin-gapped paramagnet below a nonzero critical value of $\frac{J_\perp}{J_\parallel}$. So there is a range of parameters in this 2D model where the spin-1 system is a quantum paramagnet although the spin-1/2 system has long-range Neel order.

There are some interesting examples of frustrated spin-1 magnets, most notably $NiGa_2S_4$ and $Ba_3NiSb_2O_9$, in both of which the spin-1 Ni ion forms a triangular lattice [60,61]. Apart from new and interesting kinds of quantum spin liquids, spin-1 magnets may also harbor novel broken-symmetry states (such as spin nematics [62]) more naturally than their spin-1/2 counterparts. To this we add the SPT phase discussed in this paper as a possible fate for a frustrated 3D spin-1 magnet.

Our results suggest a route to guessing possible microscopic models that might harbor an SPT phase. Starting from the parton mean-field Hamiltonian, we can write down a lattice gauge theory that captures fluctuations. A strong-coupling expansion of this lattice gauge theory will result in a spin

Hamiltonian which may then be in the same phase as the same lattice gauge theory at weaker coupling. Such an approach has previously been successfully used to write down lattice models for various spin-liquid phases. Given that we are interested here in confined phases, we may be cautiously optimistic that a similar approach has an even better chance of resulting in spin models for the SPT phases. As an application, let us consider the diamond lattice parton construction. With full SU(2) spin symmetry, the mean-field state of Sec. IV C 2 suggests [at leading order of the strong-coupling expansion in the resulting U(1) gauge theory] an interesting frustrated spin-1 model, the J_1-J_2 antiferromagnet on the diamond lattice [63]:

$$H = J_1 \sum_{\langle rr' \rangle} \vec{S}_r \cdot \vec{S}_{r'} + J_2 \sum_{\langle\langle rr' \rangle\rangle} \vec{S}_r \cdot \vec{S}_{r'}. \tag{51}$$

The next-nearest-neighbor coupling J_2 introduces frustration. Indeed, classically, once $J_2 > \frac{J_1}{8}$ there are an infinite number of degenerate ground states [64] that are not related by global spin rotation. For large spin, it has been argued that the ground state is magnetically ordered as a result of quantum order by disorder [65]. The ground state for $S = 1$ (or $S = 1/2$) is not known. The SPT paramagnet discussed in this paper is a candidate. The various descriptions we have provided should be a useful guide in future numerical studies should a paramagnetic ground state be found for this model.

It is interesting to note that—since the diamond lattice is fourfold-coordinated—classical 2-sublattice Neel order is likely to be more easily destabilized by frustration/quantum fluctuations than in the cubic lattice. Thus the J_1-J_2 diamond magnet for low spin ($S = 1/2$ or 1) may be an excellent candidate to find an interesting quantum paramagnetic ground state.

The frustrated diamond lattice model appears to describe well [64] the physics of the spinel oxide materials $MnAl_2O_4$ and $CoAl_2O_4$ [66], which belong to a general family of materials of the form AB_2O_4. The A site forms the diamond lattice and is magnetic. The Mn and Co compounds have $S = \frac{5}{2}$ and $S = \frac{3}{2}$, respectively. In searching for a material that realizes the $S = 1$ model it is natural then to consider $NiAl_2O_4$. However, this is an inverse spinel, in which the A site is instead occupied by Al and the octahedrally coordinated B site is shared randomly between Ni and Al [67]. This randomness will presumably lead to different physics in this compound.

If the regular spinel compound could be synthesized Ni would be expected to be in a d^8 Ni^{2+} configuration and would have spin-1. However, the A site is tetrahedrally coordinated, and in the resulting crystal field, the Ni^{2+} ion will have orbital degeneracy in addition to spin-1. Further spin-orbit coupling will split the resulting spin-orbital Hilbert space, and the physics of the lattice will be determined by its competition with intersite spin/orbital exchange [68]. Thus spinels with Ni atoms at the A site, even if they exist, will not simply be described by a spin-1 diamond lattice model.

Nevertheless, we hope that our considerations motivate an experimental search for and study of other frustrated spin-1 magnets.

ACKNOWLEDGMENTS

We are very grateful to A. Ramirez for bringing the fact that $NiAl_2O_4$ is an inverse spinel to our attention. A.N. thanks J. Haah and C. von Keyserlingk for useful discussions and acknowledges the support of a fellowship from the Gordon and Betty Moore Foundation under the EPiQS initiative (Grant No. GBMF4303). T.S. and C.W. acknowledge support from Grant No. NSF DMR-1305741. T.S. was partially supported by a Simons Investigator award from the Simons Foundation.

[1] P. A. Lee, Science **321**, 1306 (2008).
[2] L. Balents, Nature (London) **464**, 199 (2010).
[3] X. G. Wen, *Quantum Field Theory of Many-Body Systems* (Oxford University Press, Oxford, 2004).
[4] A. Vishwanath and T. Senthil, Phys. Rev. X **3**, 011016 (2013).
[5] F. Pollmann, A. M. Turner, E. Berg, and M. Oshikawa, Phys. Rev. B **81**, 064439 (2010); A. M. Turner, F. Pollmann, and E. Berg, *ibid.* **83**, 075102 (2011); X. Chen, Z.-C. Gu, and X.-G. Wen, *ibid.* **83**, 035107 (2011); N. Schuch, D. Pérez-Garcia, and I. Cirac, *ibid.* **84**, 165139 (2011).
[6] L. Fidkowski and A. Kitaev, Phys. Rev. B **83**, 075103 (2011).
[7] X. Chen, Z.-C. Gu, Z.-X. Liu, and X.-G. Wen, Science **338**, 1604 (2012); Phys. Rev. B **87**, 155114 (2013).
[8] A. M. Turner and A. Vishwanath, arXiv:1301.0330.
[9] T. Senthil, Annu. Rev. Con. Matt. Phys. **6**, 299 (2015).
[10] C. Wang and T. Senthil, Phys. Rev. B **87**, 235122 (2013).
[11] F. J. Burnell, X. Chen, L. Fidkowski, and A. Vishwanath, Phys. Rev. B **90**, 245122 (2014).
[12] F. Anfuso and A. Rosch, Phys. Rev. B **75**, 144420 (2007).
[13] C. Wang, A. C. Potter, and T. Senthil, Science **343**, 6171 (2014).
[14] A. Y. Kitaev, Ann. Phys. (NY) **303**, 2 (2003).
[15] The same model has also been independently studied by S. Geraedts and O. Motrunich (private communication).
[16] C. Xu, F. Wang, Y. Qi, L. Balents, and M. P. A. Fisher, Phys. Rev. Lett. **108**, 087204 (2012).
[17] I. Affleck, T. Kennedy, E. H. Lieb, and H. Tasaki, Phys. Rev. Lett. **59**, 799 (1987); Commun. Math. Phys. **115**, 477 (1988).
[18] A. Kapustin and R. Thorngren, arXiv:1309.4721.
[19] F. J. Burnell, C. W. von Keyserlingk, and S. H. Simon, Phys. Rev. B **88**, 235120 (2013).
[20] K. Walker and Z. Wang, Front. Phys. **7**, 150 (2012).
[21] C. W. von Keyserlingk, F. J. Burnell, and S. H. Simon, Phys. Rev. B **87**, 045107 (2013).
[22] X. Chen, F. Burnell, A. Vishwanath, and L. Fidkowski, arXiv:1403.6491.
[23] H. Yao, L. Fu, and X.-L. Qi, arXiv:1012.4470.
[24] C. Y. Huang, X. Chen, and F. Pollmann, Phys. Rev. B **90**, 045142 (2014).

[25] W. Li, S. Yang, M. Cheng, Z.-X. Liu, and H.-H. Tu, Phys. Rev. B **89**, 174411 (2014).

[26] X. Chen, Y.-M. Lu, and A. Vishwanath, Nat. Commun. **5**, 3507 (2014).

[27] F. Wang and C. Xu, arXiv:1110.4091.

[28] E. Fradkin, *Field Theories of Condensed Matter Physics*, 2nd ed. (Cambridge University Press, Cambridge, 2013).

[29] C. Xu and T. Senthil, Phys. Rev. B **87**, 174412 (2013).

[30] A. F. Albuquerque, F. Alet, and R. Moessner, Phys. Rev. Lett. **109**, 147204 (2012).

[31] In the pure-loop state in Sec. III, the reduced density matrix for a single sublattice is diagonal: $\rho_A \propto \sum_{\mathcal{C}_A} |\mathcal{C}_A\rangle \langle \mathcal{C}_A|$. The reduced density matrix for the AKLT-based state does not have a simple form, but by analogy we expect a suppression of off-diagonal elements. (In the artificial limit where they are completely suppressed, the spins are trivially short range correlated.)

[32] With a harmless ambiguity when the number of occupied links at a vertex exceeds two.

[33] Recall that the singlet basis allows us to represent any spin-zero state of the spin-1 system in terms of loops of spin-1/2 singlet bonds; these may form minimal length loops which backtrack on a single link, i.e., spin-1 singlet bonds, or longer AKLT loops.

[34] A. Auerbach, *Interacting Electrons and Quantum Magnetism* (Springer, New York, 1994).

[35] P. Ye and X.-G. Wen, Phys. Rev. B **87**, 195128 (2013); Y.-M. Lu and D.-H. Lee, *ibid.* **89**, 195143 (2014); T. Grover and A. Vishwanath, *ibid.* **87**, 045129 (2013).

[36] J. Oon, G. Y. Cho, and C. Xu, Phys. Rev. B **88**, 014425 (2013).

[37] P. Ye and X.-G. Wen, Phys. Rev. B **89**, 045127 (2014); M. A. Metlitski, C. L. Kane and M. P. A. Fisher (unpublished).

[38] Z. Bi, A. Rasmussen, Y. You, M. Cheng, and C. Xu, arXiv:1404.6256.

[39] A. Kitaev, AIP Conf. Proc. **1134**, 22 (2009); S. Ryu, A. P. Schnyder, A. Furusaki, and A. W. W. Ludwig, New J. Phys. **12**, 065010 (2010).

[40] L. Fidkowski, X. Chen, and A. Vishwanath, Phys. Rev. X **3**, 041016 (2013).

[41] C. Wang and T. Senthil, Phys. Rev. B **89**, 195124 (2014).

[42] M. A. Metlitski, L. Fidkowski, X. Chen, and A. Vishwanath, arXiv:1406.3032.

[43] Y.-Z. You and C. Xu, Phys. Rev. B **90**, 245120 (2014).

[44] P. Hosur, S. Ryu, and A. Vishwanath, Phys. Rev. B, **81**, 045120 (2010).

[45] A. P. Schnyder, S. Ryu, and A. W. W. Ludwig, Phys. Rev. Lett. **102**, 196804 (2009).

[46] Z.-X. Liu, Y. Zhou, H.-H. Tu, X.-G. Wen, and T.-K. Ng, Phys. Rev. B **85**, 195144 (2012).

[47] A. Y. Kitaev, Phys. Usp. **44**, 131 (2001).

[48] Any quadratic term $i\eta^{(+)T} A \eta^{(+)}$ (where A is real antisymmetric) is forbidden as it is odd under $\mathcal{T}$. However, in the presence of interactions a four-fermion term $\gamma_1\gamma_2\gamma_3\gamma_4$, where γ_i are the components of $\eta^{(+)}$ in some basis, is allowed by time reversal and lifts the boundary degeneracy to a single doublet as in the Haldane chain [69].

[49] To be more precise, the two types of generators in Eq. (29) correspond to elements of the invariant gauge group (IGG) [3] at different momenta, $k = 0$ and $k = \pi$, so when we take linear combinations, the two types of generators in Eq. (30) alternate on even and odd sites. This is not crucial here. Another subtlety is that the IGG is enlarged at the special point $\Delta = t$.

[50] This correspondence with the AKLT state is less obvious if we simply Gutzwiller project the BCS ground state of H_{MF}. The ground state of the Kitaev chain involves a long-range Cooper pair wave function, $C(r) = (L - 2r)/L$ [70], so in the present case $|\Psi_{\mathrm{spin}}\rangle$ is obtained by acting on the vacuum with an exponentiated sum of long-range singlet creation operators, $\exp(\sum_i \sum_{r>0} C(r) f_i^\dagger \sigma^y \tau^y f_{i+r}^{\dagger T})$, and projecting. The AKLT state may, of course, be written using only short-range singlet creation operators, $|\mathrm{AKLT}\rangle \propto \mathcal{P} \prod_i (f_i^\dagger \sigma^y \tau^y f_{i+1}^{\dagger T}) |\mathrm{vac}\rangle$. By the previous argument, the two states must be equivalent.

[51] M. F. Lapa, J. C. Y. Teo, and T. L. Hughes, arXiv:1409.1234.

[52] T. Senthil and M. P. A. Fisher, Phys. Rev. B **62**, 7850 (2000).

[53] L. Balents, M. P. A. Fisher, and C. Nayak, Phys. Rev. B **60**, 1654 (1999).

[54] The fermions in the bulk are confined, giving a nonfractionalized bulk state. It is known [45] that the SU(2) gauge theory has a θ term at $\theta = (\nu'/2)\pi$. For $\nu' = 4$, as here, we have $\theta = 2\pi$, which has the same physics as at $\theta = 0$. The confined state then can preserve time-reversal symmetry. In contrast, if $\nu' = 2$, we will have $\theta = \pi$, and the resulting confined phase of the SU(2) gauge theory must be nontrivial in some way. It either breaks time reversal or becomes a quantum spin liquid with long-range entanglement.

[55] The $eCTmT$ state is topologically equivalent to the combination of a generic $eTmT$ state and the state $eCmT$; the analog of the latter for U(1) spin symmetry is discussed in Sec. IV C 1.

[56] Y.-M. Lu and D.-H. Lee, arXiv:1403.5558.

[57] The symmetry is the combination of a $\pi/2$ rotation along $\hat{z}$ and a reflection $z \to -z$, followed by a particle-hole transformation $c_{\alpha,\delta,a} = \sigma^z_{\alpha\beta} \tau^z_{\delta\lambda} \gamma^z_{ab} c^\dagger_{\beta,\lambda,b}$, where $\{\alpha,\beta\}$ denote the spin, $\{\delta,\lambda\}$ denote the orbital, and $\{a,b\}$ denote the sublattice index (γ^z is a Pauli matrix acting on the sublattice indices).

[58] This electric charge couples to the emergent photon in this spin liquid and not to physical external electromagnetic fields.

[59] We must check that this does not close the gap. The total pairing term in momentum space $\Delta_{\vec{k}} + \Delta'_{\vec{k}}$ must not be positive (or negative) definite since the on-site pairing vanishes: $\langle f_{i\uparrow} f_{i\downarrow} \rangle = 0$. It is easy to show that this requires $|\Delta'| < 12|\Delta|$. One can then show that such a value of Δ' can never close the gap opened by Δ. Therefore the mean-field Hamiltonian (48) can be smoothly connected to a Hamiltonian with no Δ' term without closing the gap.

[60] S. Nakatsuji, Y. Nambu, H. Tonomura, O. Sakai, S. Jonas, C. Broholm, H. Tsunetsugu, Y. Qiu, and Y. Maeno, Science **309**, 1697 (2005).

[61] J. G. Cheng, G. Li, L. Balicas, J. S. Zhou, J. B. Goodenough, C. Xu, and H. D. Zhou, Phys. Rev. Lett. **107**, 197204 (2011).

[62] H. Tsunetsugu and M. Arikawa, J. Phys. Soc. Jpn. **75**, 083701 (2006); A. Lauchli, F. Mila, and K. Penc, Phys. Rev. Lett. **97**, 087205 (2006); S. Bhattacharjee, V. B. Shenoy, and T. Senthil, Phys. Rev. B **74**, 092406 (2006); E. M. Stoudenmire, S. Trebst, and L. Balents, *ibid.* **79**, 214436 (2009).

[63] Strictly speaking, the J_2 coupling obtained from the previous mean-field ansatz should be anisotropic. It is not clear whether this anisotropy is, in reality, essential for realizing the topological paramagnet.

[64] D. Bergman, J. Alicea, E. Gull, S. Trebst, and L. Balents, Nat. Phys. **3**, 487 (2007).

[65] J.-S. Bernier, M. J. Lawler, and Y. B. Kim, Phys. Rev. Lett. **101**, 047201 (2008).
[66] N. Tristan, J. Hemberger, A. Krimmel, H.-A. Krug von Nidda, V. Tsurkan, and A. Loidl, Phys. Rev. B **72**, 174404 (2005).
[67] R. F. Cooley and J. S. Reed, J. Am. Ceram. Soc. **55**, 395 (1972).
[68] A. Seigenfeld and T. Senthil (unpublished).
[69] E. Tang and X.-G. Wen, Phys. Rev. Lett. **109**, 096403 (2012).
[70] M. Greiter, V. Schnells, and R. Thomale, Ann. Phys. **351**, 1026 (2014).